

# Analysis of Split-Drain MAGFETs

Rodrigo Rodríguez-Torres, Edmundo A. Gutiérrez-Domínguez, *Member, IEEE*, Robert Klima, and Siegfried Selberherr, *Fellow, IEEE*

**Abstract**—We present fully three-dimensional simulation results of two-drain and three-drain magnetic field-effect transistors (MAGFETs), magnetic sensors based on metal–oxide–semiconductor field-effect transistor (MOSFET) structures. By proper development and discretization of the current density equations comprising the nonzero magnetic field components, a two-drain MAGFET is analyzed at both 77 K and 300 K. The discretization scheme is implemented in the general purpose multidimensional device and circuit simulator MINIMOS-NT which is used to investigate the relative sensitivity, the main figure of merit of any magnetic sensor, as a function of the geometric parameters and bias conditions. Besides, the physical modeling of silicon at 77 K and the Hall scattering factors for the silicon inversion layers are discussed. Our simulation results perfectly match the available experimental data. New in-depth knowledge can be obtained by simulating MOSFET structures at 77 K in the presence of an arbitrary magnetic field.

**Index Terms**—Low-temperature analysis, magnetic sensor, physical modeling, split-drain magnetic field-effect transistors (MAGFETs), three-dimensional (3-D) simulation.

## I. INTRODUCTION

CARRIER deflection of moving charges in the presence of a magnetic field is the physical phenomenon exploited in the inversion layer of MOSFET-based magnetic sensors [1]–[4]. A magnetic field perpendicular to the inversion layer can be detected either by a Hall voltage or a current imbalance, depending on which effect is maximized within the magnetic sensor body. If the inversion layer is used as a Hall plate, the Hall voltage is detected by placing contacts close to the drain terminal next to the inversion layer. Gallagher and Corak [2] have shown that such an approach does not interfere with the electric behavior of the MOSFET. Integrating the electronics and the magnetic sensor by using common IC batch fabrication techniques results in millions of identical magnetic sensors that are manufactured at very low costs, being able to detect magnetic fields in the range of a few milli-Tesla and beyond at room temperature operation.

Another approach to use the inversion layer of a MOSFET as the active area of a magnetic sensor is to split the drain contact into two or more contacts. By splitting the drain into two drain contacts, both drain contacts will equally share the current at normal bias operation when no magnetic field is applied [3],

Manuscript received April 12, 2004; revised September 23, 2004. The review of this paper was arranged by Editor K. Najafi.

R. Rodríguez-Torres, R. Klima and S. Selberherr are with the Institute for Microelectronics, Technische Universität Wien, Vienna 27-29/E360 A-1040, Austria. (e-mail: rodrigo@iue.tuwien.ac.at).

E. A. Gutiérrez-Domínguez is with the Department of Electronics, National Institute for Astrophysics, Optics, and Electronics (INAOE), Tonantzintla, Puebla, Mexico.

Digital Object Identifier 10.1109/TED.2004.839869

[5]–[8]. Ideally, the difference between both drain currents will be zero. When a magnetic field is applied perpendicular to the inversion layer, the current in the channel will be deflected as a result of the Lorentz force on the mobile charge. An imbalance in the flowing current generates a differential current that can be measured on the drain contacts and that is proportional to the magnetic field strength. The relative sensitivity of the two-drain MAGFET is defined as the ratio between this differential current and the product of the magnetic field strength with the total current

$$S = \frac{|I_{D1} - I_{D2}|}{(I_{D1} + I_{D2})|\mathbf{B}|} \quad (1)$$

where  $I_{D1}$  and  $I_{D2}$  are the currents at Drain 1 and Drain 2, and  $|\mathbf{B}|$  is the magnetic field strength.

The split-drain MAGFET has been previously investigated [9]–[13] where results show the poor sensitivity compared to their Hall plate counterparts. This can be explained in terms of (1). Because the relative sensitivity depends on the current imbalance the magnitude of which is very small compared to the magnitude of the drain currents, low relative sensitivities are obtained. As explained in [14], the magnitude of the current imbalance is related to the current deflection, defined as

$$\text{deflection} = L\mu_n|\mathbf{B}| \quad (2)$$

where  $L$  is the length of the MAGFET,  $\mu_n$  is the electron mobility in the inversion layer of a N-MOSFET, and  $|\mathbf{B}|$  is the magnetic field strength. Because applying a larger gate or drain voltage will only increase the drain currents but not the differential current, the only possibility to enlarge the differential current is to strengthen the current deflection parameters. Thus, either the device has to be long enough to produce a large deflection and then to produce a larger differential current, or the mobility of the inversion layer must be higher. In both cases the ability of the split-drain MAGFET to detect smaller magnetic fields will increase.

Split-drain MAGFETs are fully compatible with standard CMOS processes. Furthermore, CMOS technologies can operate at cryogenic temperatures (4.2 K–77 K) where the electron mobility in the inversion layer increases [15]. This effect can be advantageously exploited for the split-drain MAGFET to detect smaller magnetic fields [16]. The  $1/f$  noise, being a major drawback of the conventional MOSFET structures, is drastically reduced, yielding the possibility to detect magnetic fields in the micro-Tesla range.

## II. DISCRETIZATION SCHEME

In order to simulate galvanomagnetic effects in semiconductor materials with general purpose device simulators, the

current density equations have to be extended to take the magnetic field components into account. As proposed in [17] and [18], the current equation comprising the magnetic field in the isothermal approximation for electrons reads

$$\mathbf{J}_n = -\sigma_n(\nabla\phi_n) - \sigma_n \frac{1}{1 + (\mu_n^* \mathbf{B})^2} \{ \mu_n^* \mathbf{B} \times \nabla\phi_n \} - \sigma_n \frac{\mu_n^* \mathbf{B}}{1 + (\mu_n^* \mathbf{B})^2} \{ \mu_n^* \mathbf{B} \times (\mathbf{B} \times \nabla\phi_n) \} \quad (3)$$

where  $\sigma_n$  is the electric conductivity of the electrons,  $\nabla\phi_n$  is the gradient of the electron quasi-Fermi potential,  $\mu_n^*$  is the Hall mobility related to the drift mobility as  $\mu_n^* = r_n \mu_n$  with  $r_n$  as the Hall scattering factor and  $\mathbf{B}$  is the magnetic field.

Along with the Poisson and continuity equations (drift-diffusion approximation)

$$\text{div}(\varepsilon \cdot \text{grad } \psi) = q \cdot (n - p - C) \quad (4)$$

$$\text{div } \mathbf{J}_n = q \cdot \left( R + \frac{\partial n}{\partial t} \right) \quad (5)$$

$$\text{div } \mathbf{J}_p = -q \cdot \left( R + \frac{\partial p}{\partial t} \right) \quad (6)$$

a device can be properly simulated in the presence of a magnetic field. The discretization of (3) was carried out following the general strategy proposed by Gajewski and Gärtner [19]. The vectorial product between the current density and the magnetic field is computed by considering a local coordinate system and the neighboring points. The discretization reads

$$J_B = \frac{s_k^T (I + N^T (\beta \cdot \beta^T + \beta_\times) N^{-T}) J_0}{1 + \beta^2} \quad (7)$$

where  $J_B$  is the projected current along the mesh line in the local coordinate system which takes the magnetic field components into account,  $J_0$  is the projected current along the mesh line in the local coordinate system which does not take the magnetic field components into account,  $s_k$  is the distance ratio,  $I$  is the unitary matrix,  $\beta$  is the dimensionless product between the magnetic field and the Hall mobility,  $\beta_\times$  is a linear operator that combined with  $\beta \cdot \beta^T$  gives the matrix representation of a vectorial product, and  $N$  is the matrix composed with the unitary vectors of the local coordinate system. This discretization scheme is implemented in MINIMOS-NT [20].

The boundary conditions are not modified by the presence of a magnetic field. However, a Hall voltage appears across a device in order to compensate the deflection of the current inside the semiconductor structure. The magnitude of this Hall voltage can be very small, therefore the simulation grid should be sufficiently fine to resolve this voltage. That means, one has to have *good* knowledge of the behavior and performance of the device to efficiently design a simulation grid. For arbitrary structures this is difficult to fulfill. To circumvent this problem, a modified boundary condition can be used for the Poisson equation [21]. For general bipolar operating conditions, the isothermal case of the boundary condition for the electric potential is

$$\frac{\partial \psi}{\partial N} \Big|_{sc} = -\frac{\rho_{\text{surf}}}{\epsilon} + \sigma R_H (\mathbf{B} \times \nabla \psi) \cdot \mathbf{N} - \frac{\sigma_n^2 R_n}{\sigma} (\mathbf{B} \times \nabla (\psi - \phi_n)) \cdot \mathbf{N} + \frac{\sigma_p^2 R_p}{\sigma} (\mathbf{B} \times \nabla (\phi_p - \psi)) \cdot \mathbf{N} \quad (8)$$

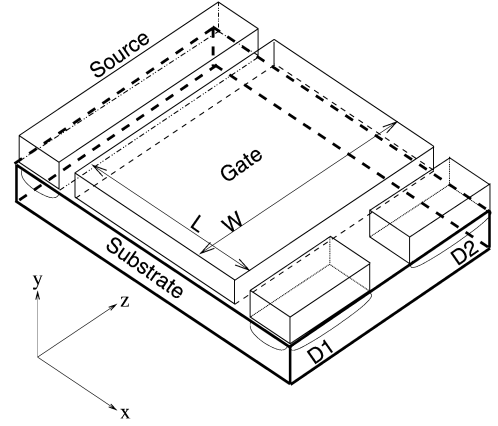


Fig. 1. View of the simulated two-drain MAGFET structure.

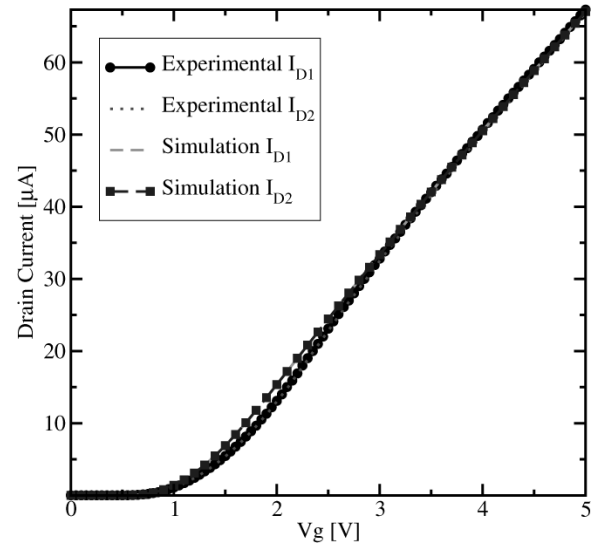


Fig. 2. Drain currents as a function of the gate voltage at 300 K.

where  $\sigma = \sigma_n + \sigma_p$  is the transversal ambipolar electric conductivity, and

$$R_H = \frac{\sigma_n^2 R_n + \sigma_p^2 R_p}{\sigma^2} \quad (9)$$

is the ambipolar Hall coefficient.

### III. TWO-DRAIN MAGFET

The simplest split-drain MAGFET structure is shown in Fig. 1, where the drain is split into two contacts. Both contacts must measure the same length, otherwise an undesirable offset will appear between both drain currents even in the case of zero magnetic field. The two-drain MAGFET structure used for the simulations has the same technology parameters as the devices fabricated in the 10  $\mu\text{m}$  CMOS INAOE MicroElectronics Laboratory [16]. It is an N-channel MOSFET with a substrate doping of  $1 \times 10^{15} \text{ cm}^{-3}$  and an oxide thickness of 60 nm. The MAGFET width is 100  $\mu\text{m}$  and the length is 125  $\mu\text{m}$ . The separation between the two drain contacts is 10  $\mu\text{m}$ . Fig. 2 shows the electrical characteristic of the MAGFET without magnetic field. The total drain current is equally shared by the drains. In Sections III-A–C, simulation results as a function of

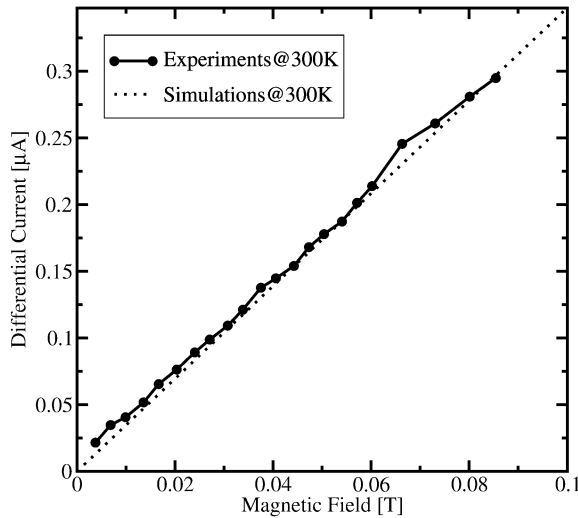


Fig. 3. Differential currents versus magnetic field at 300 K.

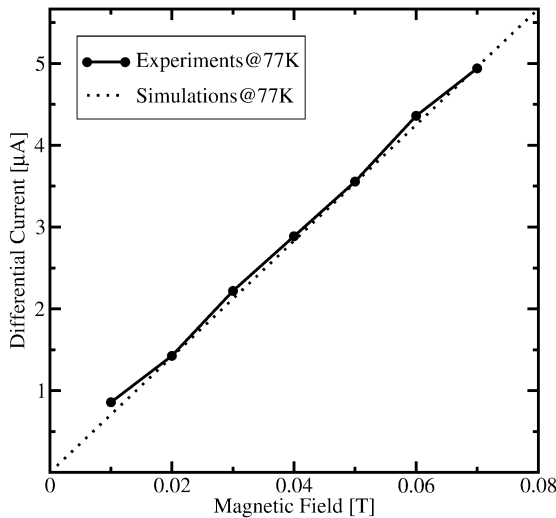


Fig. 4. Differential currents versus magnetic field at 77 K.

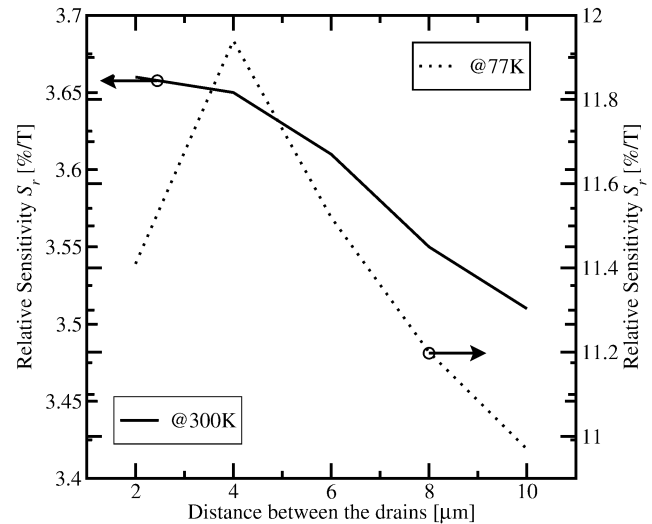
the magnetic field, geometric parameters, and polarization at both temperatures 77 K and 300 K will be given.

#### A. Differential Current versus Magnetic Field

Fig. 3 shows the experimental and simulated differential current for the structure of Fig. 1 at 300 K. The voltage at the drains is 1.0 V, the gate voltage is 4.95 V, and the bulk voltage is 0.0 V. The value of the Hall scattering factor for electrons used for the simulations is 0.6. The simulation results fit the experimental data very well. The relative sensitivity, computed according to (1), is  $2.64\% \text{ T}^{-1}$ .

Fig. 4 shows the experimental and simulated differential current for the same structure at 77 K. The bias conditions are the same as at 300 K and again the simulation results perfectly match the experimental data. The electron Hall scattering factor used for the simulation results is 0.8. The computed relative sensitivity is  $11.09\% \text{ T}^{-1}$ .

The magnitude of the Hall factor used for the simulations is quite small compared to literature data, where values between


 Fig. 5. Simulated  $S_r$  for different distances between the drains.

1.0 and 1.4 are given [17], [22]. However, as the electric characteristics with a zero magnetic field are well reproduced, we did not consider the mobility values or the MINIMOS 6 mobility model as responsible for the lack of fitting to experimental data. Thus the Hall factor is adjusted to fit the experimental data at nonzero magnetic field. Besides, the interplay of the scattering mechanisms in the inversion channel is quite complex and therefore it is not clear how to derive this Hall factor from simplifications as made for the bulk Hall factor in silicon [23]. For the following simulations, if not otherwise stated, the Hall factor for electrons has been set to 0.8.

#### B. Relative Sensitivity versus Geometric Parameters

According to [24] and [25], the structure of Fig. 1 has not the optimum geometry for a two-drain MAGFET structure. It has been identified that the distance between the drains plays a dominant role for a two-drain MAGFET. Fig. 5 shows the simulated relative sensitivity for the structure as a function of the drain separation distance  $d$ . The bias are a gate voltage of 4.95 V, 1.0 V at the drains, and 0.0 V at the substrate. The magnetic field is set to  $-50 \text{ mT}$ . The length and the width of the MAGFET are kept constant, at  $125 \mu\text{m}$  and  $100 \mu\text{m}$  respectively. At 300 K, the relative sensitivity increases from  $3.51\% \text{ T}^{-1}$  at  $d = 10 \mu\text{m}$  to  $3.66\% \text{ T}^{-1}$  at  $d = 2 \mu\text{m}$ .

At 77 K the relative sensitivity increases from  $3.51\% \text{ T}^{-1}$  at room temperature to  $10.97\% \text{ T}^{-1}$  at  $d = 10 \mu\text{m}$ , which represents an enhancement in magnetic sensitivity of more than 300%. This enhancement is attributed to the increase in the carrier mobility due to the reduction of phonon scattering. A maximum of  $11.94\% \text{ T}^{-1}$  in the relative sensitivity at 77 K is observed at  $d = 4 \mu\text{m}$  and then the relative sensitivity reduces at  $d = 2 \mu\text{m}$ . If the values of relative sensitivity between  $d = 4 \mu\text{m}$  and  $d = 10 \mu\text{m}$  are interpolated, a relative sensitivity of  $12.5\% \text{ T}^{-1}$  is expected, which is larger than the theoretical limit of  $12\% \text{ T}^{-1}$  for a mobility value of more than  $15\,000 \text{ cm}^2/\text{Vs}$  [4].

The previous results show that the relative sensitivity improves, because the mobility increases as the operation temperature decreases. However, there is another parameter that can be modified in order to improve the relative sensitivity: The length

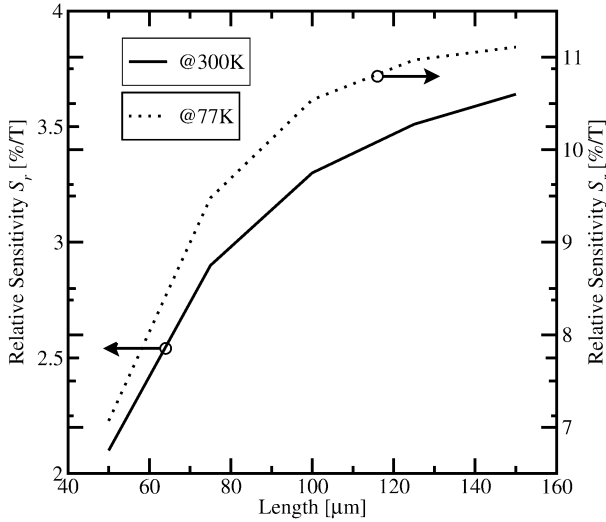


Fig. 6. Simulated relative sensitivity for different lengths.

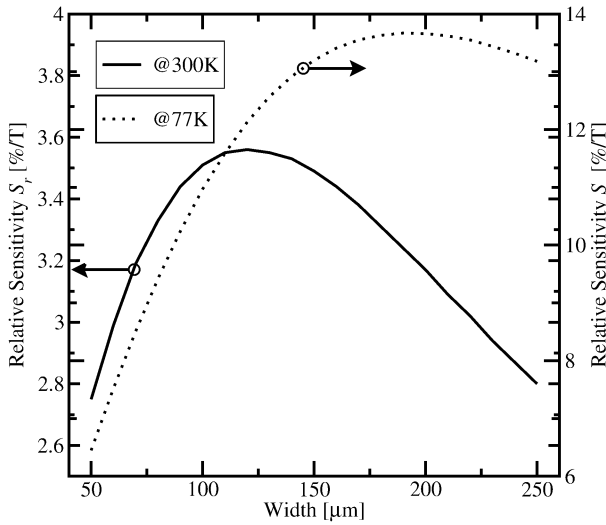


Fig. 7. Simulated relative sensitivity for different widths.

of the MAGFET. Fig. 6 shows how the relative sensitivity improves if the length of the MAGFET is increased from  $50 \mu\text{m}$  to  $150 \mu\text{m}$ . The bias are a gate voltage of  $4.95$  and  $1.0$  V at the drains and  $0.0$  V at the substrate. The magnetic field is set to  $-50$  mT. The width and  $d$  distance are kept constant at  $100 \mu\text{m}$  and  $10 \mu\text{m}$  respectively. At  $300$  K, the relative sensitivity increases from  $2.10\% \text{ T}^{-1}$  to  $3.64\% \text{ T}^{-1}$ . However, at  $77$  K the relative sensitivity improves from  $7.07\% \text{ T}^{-1}$  to  $11.11\% \text{ T}^{-1}$ .

Fig. 7 shows the simulated relative sensitivity as a function of the width. The bias is a gate voltage of  $4.95$ , and  $1.0$  V at the drains, and  $0.0$  V at the substrate. The magnetic field is set to  $-50$  mT. The length and  $d$  distance are kept constant at  $125$  and  $10 \mu\text{m}$ , respectively. At  $300$  K, the relative sensitivity increases from  $2.75\% \text{ T}^{-1}$  to a maximum of  $3.56\% \text{ T}^{-1}$  at a width of  $120 \mu\text{m}$ . However, at  $77$  K, the relative sensitivity increases from  $6.45\% \text{ T}^{-1}$  to a maximum of  $13.67\% \text{ T}^{-1}$  at a width of  $190 \mu\text{m}$ . The fact that both maxima are not at the same width can be explained in terms of the cryogenic operation of the MOSFET, where the increase in the carrier mobility changes the distance where the carriers are deflected, and thus the maximum occurs for a different geometry.

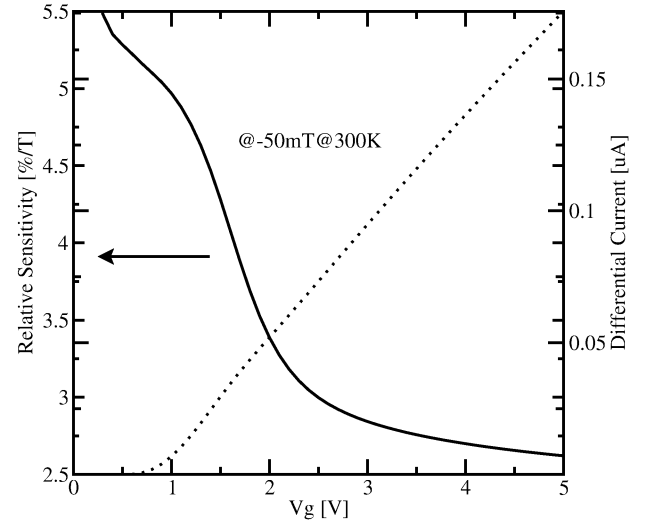


Fig. 8.  $S_r$  and  $\Delta$  as a function of  $V_G$ .  $V_{D1}$  and  $V_{D2}$  are set to  $1.0$  V.

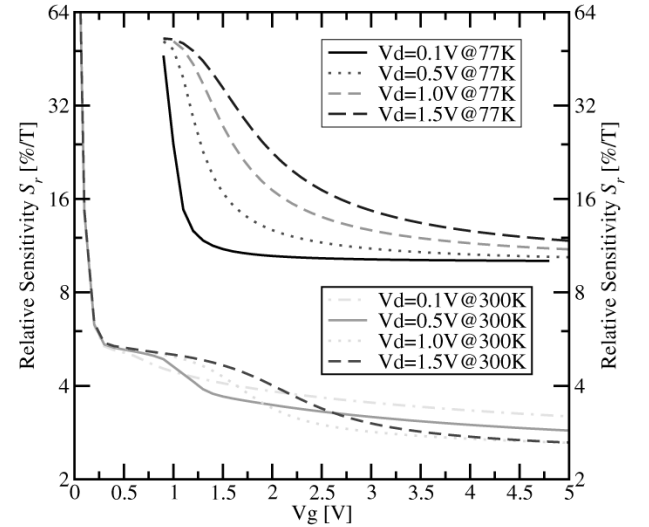


Fig. 9.  $S_r$  as a function of the gate voltage at  $B = -50$  mT.

### C. Relative Sensitivity versus Polarization

The polarization of the MAGFET is relevant for the determination of the Hall voltage. The Hall voltage depends on the carrier concentration and the thickness of the inversion layer [2]. However, the relative sensitivity depends on the differential current between the drain contacts as described by (1). Fig. 8 shows the simulated relative sensitivity and the differential current as a function of the gate voltage for the two-drain MAGFET with a length of  $125 \mu\text{m}$ , a width of  $100 \mu\text{m}$ , and  $d = 10 \mu\text{m}$ . The increase in the differential current does not give an increase in the relative sensitivity. This can be explained in terms of the current magnitudes. The differential current is only a few microamperes whereas the drain currents are at least two orders of magnitude higher.

The relative sensitivity should depend on the drain to source voltage because this voltage modulates the thickness of the inversion layer. Fig. 9 shows the simulation results of this dependence for various drain voltages at  $77$  K and  $300$  K. The relative sensitivity is much higher when the MAGFET structure is operated at  $77$  K, where a *linear* behavior with respect to

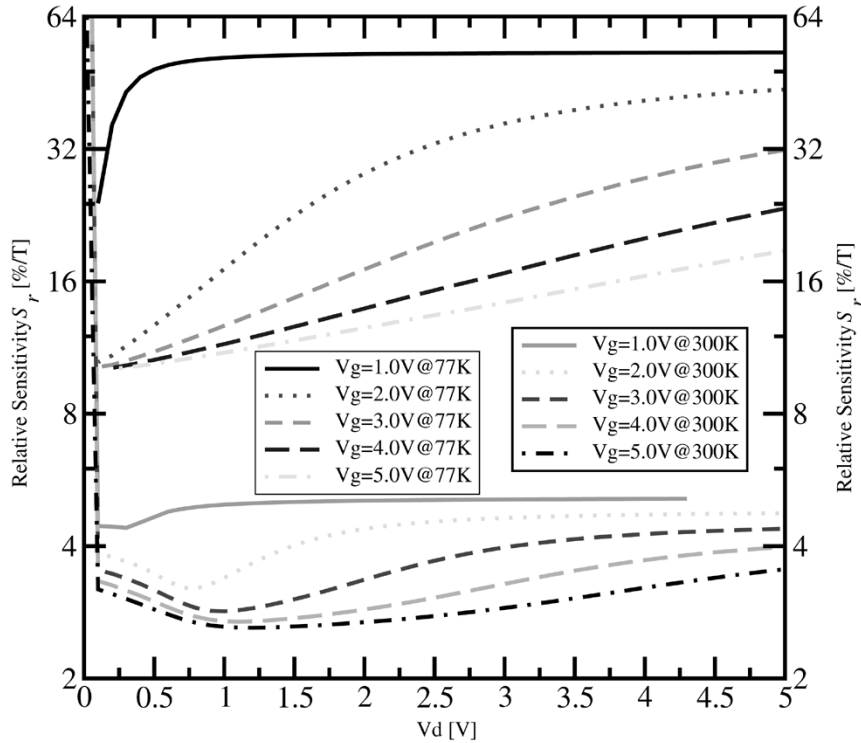


Fig. 10.  $S_r$  as a function of the drain voltage at  $B = -50$  mT.

the gate and drain polarization can be observed. Note, how the relative sensitivity at 300 K shows a complex behavior which can be explained in terms of how the carriers move inside the channel. At very low drain and gate voltages, diffusion of carriers is the dominant mechanism, while at high gate and drain polarizations, drift is the dominant mechanism. In the transition from diffusion to drift both mechanisms play a role. At 77 K, charge diffusion reduces at very low polarizations, and, as can be seen from Fig. 9, below gate voltages of 1.0 V, the current is nearly zero. The simulations of the relative sensitivity at 77 K show that as the drain and gate voltage increase, the relative sensibility increases too. At 300 K the relative sensibility saturates at a value of  $2.62\% T^{-1}$  for a Hall factor for electrons of 0.6.

The transition between the drift and diffusion regimes can explain the *s*-shape of the relative sensitivity at 300 K in Fig. 9. Fig. 10 shows how the relative sensitivity varies as a function of the drain voltage for different gate voltages at 77 K and 300 K. The various minima at 300 K can be seen as the transition between the linear and the saturation operation region of the MOSFET. At 77 K no minima are observed, because diffusion is of minor importance at cryogenic MOSFET operation. As seen in Fig. 9 the improvement in the relative sensibility is very high.

#### IV. THREE-DRAIN MAGFET

The concept of the three-drain MAGFET is as old as the MOS Hall plate device [2]. It was first proposed in [9], [26] where it is suggested to bound together the Hall voltage terminals and the drain to form a three-drain MAGFET. As stated by Gallagher [2], in a MOS Hall plate device the Hall voltage terminals should be placed as close as possible to the drain terminal in order to

detect the Hall voltage and not to interfere with the electrical behavior of the MOSFET. That is the reason why in [9], [26] the proposal of a three-drain MAGFET using Hall plates has been given. By taking the central drain current as a reference, a differential current can be measured on the lateral drains. However, no simulation results or experimental data showing the three-drain MAGFET as a magnetic sensor with a differential current output have been published yet. Therefore, based on the successful simulations of a two-drain MAGFET, a three-drain MAGFET structure is analyzed. In the following some simulation results are given.

Fig. 11 shows the three-drain MAGFET structure. The main difference between the two-drain and three-drain MAGFET is the central drain current at the three-drain MAGFET. The relative sensitivity is defined as follows:

$$S_r = \frac{|I_{D1} - I_{D3}|}{(I_{D1}^0 + I_{D2}^0 + I_{D3}^0) |\mathbf{B}|} \quad (10)$$

where  $I_{D1}$  and  $I_{D3}$  are the currents at Drain 1 and Drain 3 when the magnetic field is applied,  $I_{D1}^0$ ,  $I_{D2}^0$ , and  $I_{D3}^0$  are the drain currents when the magnetic field is not applied, and  $|\mathbf{B}|$  is the magnetic field. Because the definition of the relative sensitivity is related to the total current in the detection process, one has to take into account the whole drain current. Taking only the central drain current will give unrealistically high relative sensitivities. *A priori* it is possible to conclude that reducing the reference current will lead to higher relative sensitivities, as it can be seen from Fig. 12.

The three-drain MAGFET has been simulated with the same technological parameters as the two-drain MAGFET structure. The length is  $125 \mu\text{m}$ , the width is  $80 \mu\text{m}$ , and the distance between the drains is  $10 \mu\text{m}$ . The drain voltages are 1.0 V, the gate voltage is 4.95 V, and the substrate voltage is 0.0 V. The

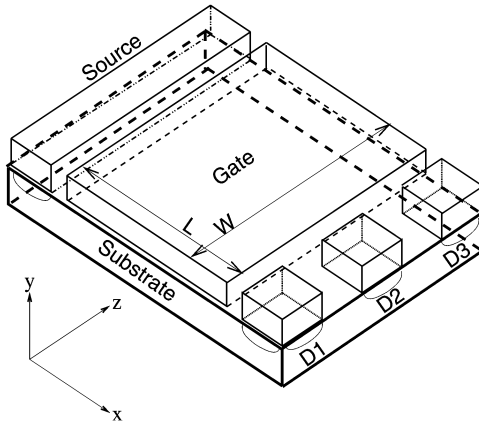


Fig. 11. View of the simulated three-drain MAGFET structure.

magnetic field is set to  $-50$  mT. A tendency cannot be deduced from Fig. 12 unless the magnitude of the drain currents for the zero magnetic field are analyzed. For a central drain size of  $12 \mu\text{m}$  a maximum in the relative sensitivity of  $4.56\% \text{ T}^{-1}$  at  $300$  K and  $13.00\% \text{ T}^{-1}$  at  $77$  K are observed. The magnitude of the central drain current is nearly 60% of the lateral drain currents at  $300$  K ( $I_{D2} = 20.86 \mu\text{A}$  and  $I_{D1,3} = 34.60 \mu\text{A}$ ) and about 44% at  $77$  K ( $I_{D2} = 56.93 \mu\text{A}$  and  $I_{D1,3} = 133.70 \mu\text{A}$ ).

Because the magnitude of the reference current is small, the relative sensitivity is high, according to expression (10). However, the magnitude of the central drain current cannot be set as a general rule because the central drain current for the drain size of  $8 \mu\text{m}$  is high as for the lateral drain currents and it gives a reasonable high relative sensitivity at both  $300$  K and  $77$  K.

The geometric dependence of the relative sensitivity for the three-drain MAGFET follows the same laws as for the two-drain MAGFET. The important characteristic of the three-drain MAGFET is that the central drain current should be as small as possible, but one has to guarantee that the side drain currents are equal, otherwise, an undesired offset will impact the general performance of three-drain MAGFETs, as seen in the following simulations.

Fig. 13 shows the simulated relative sensitivity as a function of the gate voltage for different drain voltages at  $77$  K and  $300$  K. An improvement of two times in the relative sensitivity can be obtained at  $300$  K, if the MAGFET is split in three drains in such a way that the central drain current is as small as possible. The three-drain MAGFET has the following geometric parameters: A length of  $125 \mu\text{m}$ , a width of  $80 \mu\text{m}$ , a distance between the drains of  $10 \mu\text{m}$ , and the central drain measures  $12 \mu\text{m}$ .

Fig. 14 shows the simulated relative sensitivity as a function of the drain voltage for different gate voltages at  $77$  K and  $300$  K. Even for very high voltages, where the relative sensitivity is very low, the three-drain MAGFET gives a superior performance with respect to the two-drain case at  $300$  K. One can expect an incredible improvement of the relative sensitivity for the three-drain MAGFET when operated at  $77$  K. From Figs. 9 and 13 and Figs. 10 and 14, it is clear that the two-drain MAGFET performs twice as good as the three-drain MAGFET. A plausible explanation can be given in terms of the current magnitudes: at low temperature operation they increase considerably. There-

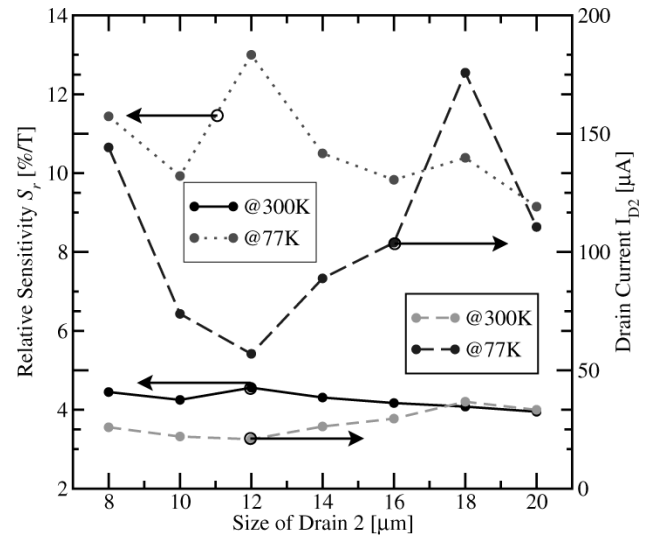


Fig. 12. Simulated  $S_r$  and  $I_{D2}$  for different sizes of Drain 2.

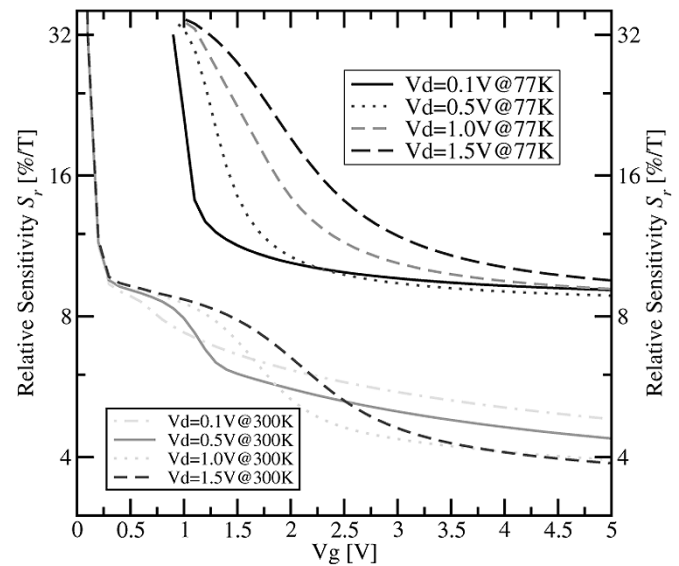


Fig. 13.  $S_r$  as a function of the gate voltage at  $B = -50$  mT.

fore, the gain in the differential current is lost by the magnitude of the reference current.

## V. PHYSICAL MODELING AT $77$ K

From a historical point of view, MINIMOS-NT has been designed in such a way that the large numerical differences between the quantities to be solved, the electric potential and carrier concentrations, do not interfere with the numerical solver when a device is simulated at temperatures different to room temperature [27]. However, not only the numerical differences impact the modeling of semiconductor devices at low temperatures. As pointed out in [15] and [28], physical parameters as the intrinsic carrier concentration, band-gap energy, or mobility values differ. According to our simulation experience [29], the electric characteristics of the two-drain MAGFET, the device for which experimental data at  $77$  K are available, are well reproduced by MINIMOS-NT. However, that does not mean that all physical models available in the simulator properly repro-

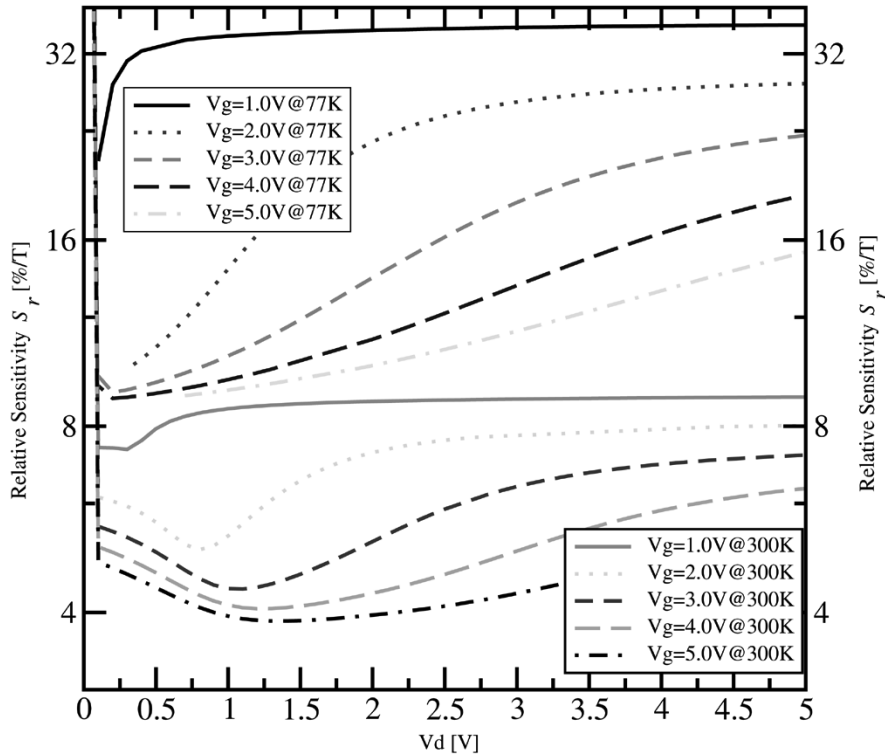


Fig. 14.  $S_r$  as a function of the drain voltage at  $B = -50$  mT.

duce all physical effects in the temperature range of cryogenic interest: 4.2 K to 77 K. For example, the MINIMOS-NT mobility model only takes lattice, ionized-impurity, and surface scattering together with velocity saturation into account. At 77 K neutral impurity scattering freezes some donor (or acceptor) atoms, lowering the concentration of available carriers for the electric conduction. Carrier to carrier scattering is important at very small dimensions, where large carrier concentrations are located in very small volumes. At 77 K, the carrier concentrations are highly concentrated in very small volumes due to quantum-mechanical effects, no matter what the device dimensions are. All of this impacts the inversion layer of MOSFET devices. However, as long as the electrical characteristics of nanometer MOSFET devices are well reproduced even at 77 K, mobility models taking into account missing scattering mechanisms at cryogenic temperatures will be developed only for fundamental physics research.

The simulation results that have been presented in this work have been computed using a small numerical value for the electron Hall factor. During the implementation of (3) by using the discretization scheme (7), simulations of small dies in the presence of a magnetic field have been performed. The simulated Hall voltages agree with the analytical values when a Hall factor of 1.1 for electrons and 0.7 for holes are used. The Hall voltages agree with the analytical values even in the case when the spatial direction of the current density and magnetic field varies. In view that the electrical characteristics of the two-drain MAGFET are well reproduced at both 77 K and 300 K, and that the magnetic effects are well reproduced by using smaller values of the Hall factors, this indicates that more research in the physical modeling at both 77 K and 300 K is needed, although the

simulation results do reproduce the available experimental data very well.

## VI. STATE OF THE ART MAGNETIC SENSORS

Superconducting quantum interface devices, better known as SQUIDS, are by far the most sensitive magnetometers ever made [30]–[32]. Their incredible resolution and very low noise make them the perfect choice for biomagnetism measurements where very low magnetic fields are present [33]. However, SQUIDS must be operated at the temperature of liquid Helium (4.2 K) for optimal operation [34] making SQUIDS massive devices with expensive operation costs. Although recent development in high temperature SQUIDS has been made [35], [36], advances in flux gate magnetometers show sensitivities which can compete with high temperature SQUIDS [37]. Also, magnetic sensors based on the anisotropic magnetoresistance effect, the giant magnetoresistance effect, or compound semiconductors have high sensitivities [38]–[40].

All of those devices are manufactured using noncompatible steps of semiconductor processes, making it difficult to integrate sensor and electronics on the same substrate. The great advantage of the MAGFET is that is 100% compatible with the standard CMOS process. This feature has been advantageously used in the following [41]–[44] where in spite of its weakness, the split-drain MAGFET has been used as the transducer of the application at room temperature operation. As a novel application in a CMOS system, a split-drain MAGFET can be used to test the signal integrity of a data line [45]. It is clear that full understanding of the split-drain MAGFET under such operating conditions requires full three-dimensional analysis of the sensor.

Up to now our device has been tested *as it is*, that is, as a single device with no integrated electronics for temperature compensation or noise reduction. At room temperature operation the split-drain MAGFET is a high-field sensing device with a sensing range in the order of mT, but when operated at 77 K, the split drain MAGFET classifies as a medium-field sensing device with a sensing range in the order of nT [16], [31], [32]. At 77 K, the two-drain MAGFET has a sensitivity of  $80 \mu\text{T}$  that is far away from the high temperature  $\text{YBa}_2\text{Cu}_3\text{O}_7$  SQUID which has a sensitivity of 20 pT [46]. Implementing a noise reduction strategy, the split-drain MAGFET can reach a sensitivity of 50 nT. An obvious advantage of the operation of CMOS systems at 77 K is that the thermal noise is reduced, whereas the flicker noise remains fairly temperature independent [15]. The noise level of the two-drain MAGFET is  $88 \text{ nV}/\sqrt{\text{Hz}}$  at 100 Hz at 77 K and the measured offset is of 31 nA at 77 K. We expect that the split-drain MAGFET integrated with electronics and operated at 77 K achieves competitive sensitivities and noise levels.

## VII. CONCLUSION

Full geometrical analyzes of two-drain and three-drain MAGFETs have been carried out. Rigorous three-dimensional simulations have been carried out to investigate the relative sensitivity of both structures at 77 K and 300 K. Results show that square structures with larger lengths offer higher relative sensitivity at room temperature operation, but wider devices give better relative sensitivities at cryogenic temperature operation. In addition it is shown that the polarization of the split-drain MAGFET structure exhibits a complex behavior at 300 K whereas at 77 K it is very simple.

Three-drain MAGFET structures perform better compared to two-drain MAGFET structures at room temperature. The central drain current should be as small as possible in order to get a higher relative sensitivity. However, a mismatch for the side drain currents of a three-drain MAGFET could be the disadvantage of this structure. Also, it has been shown that split-drain MAGFET structures operated at cryogenic temperatures can be used as magnetic sensors where high resolution and low noise are needed, for example, geomagnetic measurements.

## REFERENCES

- [1] A. C. Beer, "The Hall effect and related phenomena," *Solid State Electron.*, vol. 9, no. 5, pp. 339–351, May 1966.
- [2] R. C. Gallagher and W. S. Corak, "A metal-oxide-semiconductor (MOS) Hall element," *Solid State Electron.*, vol. 9, no. 5, pp. 571–580, May 1966.
- [3] H. P. Baltes and R. S. Popović, "Integrated semiconductor magnetic field sensors," *Proc. IEEE*, vol. 74, pp. 1107–1132, Aug. 1986.
- [4] S. M. Sze, *Semiconductor Sensors*: Wiley, 1994.
- [5] R. S. Popović and H. P. Baltes, "A CMOS magnetic-field sensor," *IEEE J. Solid-State Circuits*, vol. 18, no. 4, pp. 426–428, Aug. 1983.
- [6] A. Nathan, L. Andór, H. P. Baltes, and H. G. Schmidt-Weinmar, "Modeling of a dual-drain NMOS magnetic-field sensor," *IEEE J. Solid-State Circuits*, vol. 20, no. 3, pp. 819–821, June 1985.
- [7] A. Nathan, A. M. J. Huizer, and H. P. Baltes, "Two-dimensional numerical modeling of magnetic-field sensors in CMOS technology," *IEEE Trans. Electron Devices*, vol. ED-32, pp. 1212–1219, July 1985.
- [8] L. Andór, H. P. Baltes, A. Nathan, and H. G. Schmidt-Weinmar, "Numerical modeling of magnetic-field sensitive semiconductor devices," *IEEE Trans. Electron Devices*, vol. ED-32, pp. 1224–1230, July 1985.
- [9] A. Chovet, C. S. Roumenin, G. Dimopoulos, and N. Mathieu, "Comparison of noise properties of different magnetic-field semiconductor integrated sensors," *Sens. Actuators A, Phys.*, vol. A22, no. 1–3, pp. 790–794, Mar. 1990.
- [10] N. Mathieu, P. Giordano, and A. Chovet, "Si MAGFETs optimized for sensitivity and noise properties," *Sens. Actuators A, Phys.*, vol. 32, no. 1–3, pp. 656–660, Apr. 1992.
- [11] J. Lau, P. K. Ko, and P. C. Chan, "Modeling of split-drain magnetic field-effect transistor (MAGFET)," *Sens. Actuators A, Phys.*, vol. 49, no. 3, pp. 155–162, July 1995.
- [12] Y. A. Chaplygin, A. I. Galushkov, I. M. Romanov, and S. I. Volkov, "Experimental research on the sensitivity and noise level of bipolar and CMOS integrated magnetotransistors and judgement of their applicability in weak-field magnetometers," *Sens. Actuators A, Phys.*, vol. A49, no. 3, pp. 163–166, July 1995.
- [13] D. Killat, J. v. Kluge, F. Umbach, W. Langheinrich, and R. Schmitz, "Measurement and modeling of sensitivity and noise of MOS magnetic field-effect transistors," *Sens. Actuators A, Phys.*, vol. 61, no. 1–3, pp. 346–351, June 1997.
- [14] R. Rodríguez-Torres, E. A. Gutiérrez-Domínguez, R. Klima, and S. Selberherr, "Three-dimensional analysis of a MAGFET at 300 K and 77 K," in *Proc. Eur. Solid-State Device Research Conf.*, G. Baccarani, E. Gnani, and M. Rudan, Eds., Sept. 2002, pp. 151–154.
- [15] E. A. Gutiérrez-Domínguez, M. J. Deen, and C. L. Claeys, *Low Temperature Electronics: Physics, Devices, Circuits and Applications*, New York: Academic, 2001.
- [16] E. A. Gutiérrez-D., R. S. Murphy-A, A. Torres-J., M. Linares-A., P. J. García-R., R. Rojas-H., and V. Páez-V, "A sub-mT cryogenic silicon magnetic sensor," in *Proc. Eur. Solid-State Device Research Conf.*, A. Touboul, Y. Danto, J. Klein, and H. Grünbacher, Eds., Sept. 1998, pp. 188–191.
- [17] C. Jungemann, D. Dudenbostel, and B. Meinerzhagen, "Hall factors of Si NMOS inversion layers for MAGFET modeling," *IEEE Trans. Electron Devices*, vol. 46, pp. 1803–1804, Aug. 1999.
- [18] G. K. Wachutka, "Unified framework for thermal electrical, magnetic, and optical semiconductor device modeling," *COMPEL*, vol. 10, no. 4, pp. 311–321, Oct. 1991.
- [19] H. Gajewski and K. Gärtner, "On the discretization of van Roosbroeck's equations with magnetic field," *ZAMM*, vol. 76, no. 5, pp. 247–264, May 1996.
- [20] *Minimos-NT Device and Circuit Simulator*, 2nd ed., Institute for Microelectronics, Vienna, Austria, 2002.
- [21] C. Riccobene, "Multidimensional analysis of galvanomagnetic effects in magnetotransistors," Ph.D. dissertation, Eidgenössische Technische Hochschule Zürich, Zurich, Switzerland, 1995.
- [22] D. R. Briglio, A. Nathan, and H. P. Baltes, "Measurement of Hall mobility in N-channel silicon inversion layer," *Can. J. Phys.*, vol. 65, no. 8, pp. 842–845, Aug. 1987.
- [23] K. Seeger, *Semiconductor Physics: An Introduction*. New York: Springer-Verlag, 1989.
- [24] P. J. G. Ramírez, "Análisis, modelado y diseño de una estructura split-drain MAGFET bajo condiciones de operación a 77 K y 300 K," Ph.D. dissertation, Instituto Nacional de Astrofísica, Óptica y Electrónica, Tonantzintla, Puebla, Mexico, 2000.
- [25] J. W. A. von Kluge and W. A. Langheinrich, "An analytical model of MAGFET sensitivity including secondary effects using a continuous description of the geometric correction factor  $G$ ," *IEEE Trans. Electron Devices*, vol. 46, pp. 89–95, Jan. 1999.
- [26] S. Kordić, "Integrated silicon magnetic-field sensors," *Sens. Actuators*, vol. 10, no. 3–4, pp. 347–378, Nov./Dec. 1986.
- [27] S. Selberherr, "MOS device modeling at 77 K," *IEEE Trans. Electron Devices*, vol. 36, pp. 1464–1474, Aug. 1989.
- [28] F. Balestra and G. Ghibaudo, *Device and Circuit Cryogenic Operation for Low Temperature Electronics*. Norwell, MA: Kluwer, 2001.
- [29] R. R. Torres, "Three-dimensional simulations of split-drain MAGFETs," Ph.D. dissertation, Tech. Univ. Wien, Vienna, Austria, 2003.
- [30] J. Clarke, "Principles and applications of SQUIDS," *Proc. IEEE*, vol. 77, pp. 1208–1223, Aug. 1989.
- [31] J. E. Lenz, "A review of magnetic sensors," *Proc. IEEE*, vol. 78, pp. 973–989, June 1990.
- [32] A. E. Mahdi, L. Panina, and D. Mapps, "Some new horizons in magnetic sensing: high- $T_c$  SQUIDS, GMR and GMI materials," *Sens. Actuators A, Phys.*, vol. 105, no. 3, pp. 271–285, Aug. 2003.
- [33] D. J. Mapps, "Remote magnetic sensing of people," *Sens. Actuators A, Phys.*, vol. 106, no. 1–3, pp. 321–325, Sept. 2003.

- [34] C. Granata, A. Monaco, C. D. Russo, M. P. Lissitski, and M. Russo, "Temperature dependence performances of fully integrated DC SQUID magnetometers," *IEEE Trans. Appl. Superconduct.*, vol. 13, pp. 3829–3832, Dec. 2003.
- [35] I.-S. Kim, K. K. Yu, Y. H. Lee, H. C. Kwon, and Y. K. Park, "Performance of high- $T_c$  SQUID magnetometers for application in biomagnetism," *IEEE Trans. Appl. Superconduct.*, vol. 13, pp. 352–355, June 2003.
- [36] H.-J. Barthelmeß, M. Halverscheid, B. Schiefenhövel, E. Heim, M. Schilling, and R. Zimmermann, "Low-noise biomagnetic measurements with a multichannel DC-SQUID system at 77 K," *IEEE Trans. Appl. Superconduct.*, vol. 11, pp. 657–660, Mar. 2001.
- [37] P. Ripka, "Advances in fluxgate sensors," *Sens. Actuators A, Phys.*, vol. 106, no. 1–3, pp. 8–14, Sept. 2003.
- [38] D. Robbes, C. Dolabdjian, S. Saez, Y. Monfort, G. Kaiser, and P. Ciureanu, "Highly sensitive uncooled magnetometers: State of the art. Superconducting magnetic hybrid magnetometers, an alternative to SQUIDs?," *IEEE Trans. Appl. Superconduct.*, vol. 11, pp. 629–634, Mar. 2001.
- [39] M. Vopálenký, P. Ripka, and A. Platil, "Precise magnetic sensors," *Sens. Actuators A, Phys.*, vol. 106, no. 1–3, pp. 38–42, Sept. 2003.
- [40] N. Haned and M. Missous, "Nano-tesla magnetic field magnetometry using an InGaAs-AlGaAs-GaAs 2DEG Hall sensor," *Sens. Actuators A, Phys.*, vol. 102, no. 3, pp. 216–222, Jan. 2003.
- [41] G. Busatto, R. L. Capruccia, F. Iannuzzo, F. Velardi, and R. Roncella, "An on chip non invasive integrated current sensing," in *Proc. 6th Int. Seminar Power Semiconductors*, 2002, pp. 121–124.
- [42] K. Nakano, T. Takahashi, and S. Kawahito, "A CMOS smart rotary encoder using magnetic sensor arrays," in *Proc. Sensors*, 2003, pp. 206–209.
- [43] C.-H. Kuo, S.-L. Chen, L.-A. Ho, and S.-I. Liu, "CMOS oversampling  $\Delta\Sigma$  magnetic-to-digital converters," *IEEE J. Solid-State Circuits*, vol. 36, pp. 1582–1586, Oct. 2001.
- [44] P. Malcovati and F. Maloberti, "An integrated microsystem for 3-D magnetic field measurements," *IEEE Trans. Instrum. Meas.*, vol. 49, pp. 341–345, Apr. 2000.
- [45] H. Kim, D. M. H. Walker, and D. Colby, "A practical built-in current sensor for IDDQ testing," in *Proc. IEEE Int. Test Conf.*, 2001, pp. 405–414.
- [46] L. A. Knauss, A. B. Cawthorne, N. Lettsome, S. Kelly, F. C. Wellstood, and W. E. V. D. Linde, "Scanning SQUID microscopy for current imaging," *Microelectron. Reliabil.*, vol. 41, pp. 1211–1229, 2001.



**Rodrigo Rodríguez-Torres** was born in Huajuapán de León, Oaxaca, México, in 1972. He received the Ingeniero Industrial en Electrónica degree in electrical engineering from the Technical Institute of Puebla, Puebla, Mexico, in 1994, the M.S. and Ph.D. degrees from the National Institute for Astrophysics, Optics and Electronics (INAOE), Tonantzintla, Puebla, in 1997 and 2002, respectively, and the Ph.D. degree in technical sciences from the Institute for Microelectronics, Technische Universität Wien, in 2003.

His scientific interests include the modeling of physical effects in semiconductors, MOSFET device modeling, and device and circuit simulation.



**Edmundo A. Gutiérrez-Domínguez** (M'95) was born in Mexicali, Baja California, México, in 1960. He received the Licenciatura en Electrónica degree from the Autonomous University of Puebla, Puebla, Mexico, in 1986, the M.S. degree from the National Institute for Astrophysics, Optics, and Electronics (INAOE), Tonantzintla, Puebla, in 1987, and the Ph.D. degree in electronics sciences from the Catholic University of Leuven, Leuven, Belgium, in 1993.

He has been a Guest Researcher at IMEC, Leuven, Belgium; the Engineering School, Simon Fraser University, Vancouver, BC, Canada; Sao Paulo University, Sao Paulo, Brazil; and the Institute for Microelectronics, Vienna University of Technology, Vienna, Austria. From 1999 to 2000, he was appointed Head of the Department of Electronics, INAOE, and from 2000 to 2002 he was Director of the Motorola Design Center, Puebla. Currently, he is a Researcher at the INAOE. His research activities are focused in the microelectronics field: semiconductor device physics and technology, SiGe integrated circuit design, silicon micromachining, and solid-state sensors compatible with IC fabrication techniques.



**Robert Klima** was born in Vienna, Austria, in 1969. He received the Diplomingenieur degree in electrical engineering and the Ph.D. degree in technical sciences from the Technische Universität Wien, Vienna, Austria in 1997 and 2002, respectively.

He joined the Institute for Microelectronics, Technische Universität Wien, in 1997 focusing on three-dimensional effects in new semiconductor structures. His scientific interests include device and circuit simulation, computer visualization, and software technology.



**Siegfried Selberherr** (F'93) was born in Klosterneuburg, Austria, in 1955. He received the Diplomingenieur degree in electrical engineering and the Ph.D. degree in technical sciences from the Technische Universität Wien, Vienna, Austria, in 1978 and 1981, respectively.

He has been holding the *venia docendi* on computer-aided design since 1984. Since 1988 he has been the head of the Institute for Microelectronics, Technische Universität Wien, and since 1999, he has been Dean of the Faculty of Electrical Engineering and Information Technology. His current topics are modeling and simulation of problems for microelectronics engineering.